



An interpretable deep learning strategy for effective thermal conductivity prediction of porous materials

Qingfu Huang, Donghui Hong, Bo Niu, Donghui Long^{*}, Yun Zhang^{*}

Key Laboratory for Specially Functional Materials and Related Technology of the Ministry of Education, East China University of Science and Technology, Shanghai 200237, China



ARTICLE INFO

Keywords:

Porous materials
Effective thermal conductivity
Interpretable deep learning
Feedback

ABSTRACT

The effective thermal conductivity of porous materials plays a pivotal role in advancing novel thermal insulation materials. Existing theoretical prediction methods are computationally demanding with restricted applicability, and deep learning methods lack interpretability. More importantly, current approaches fail to explore the material structures themselves and leverage those insights to improve the accuracy of thermal conductivity prediction. Herein, we for the first time propose an interpretable deep learning approach with feedback for thermal conductivity prediction. A 3D convolutional neural network is trained on material structures-thermal conductivity data, and heat maps are generated from weighted feature maps to elucidate the prediction processes. Through image processing, incongruous regions are eliminated, resulting in porous structures with improved reasonability. Consequently, more accurate effective thermal conductivities can be obtained. This work may offer a novel predictive approach that refines both the material structure and the predictive model, thereby achieving more precise thermal conductivity predictions for porous materials.

1. Introduction

Porous materials consist of solid and pore phases embedded within a matrix, presenting distinct characteristics compared to continuous media. The elevated specific surface area [1], tenable pore sizes and morphologies, enable them with diverse applications in a wide range of fields, such as in adsorption, separation and thermal resistance processes [2]. Porous materials are ideal thermal insulators owing to their low thermal conductivity resulting from the pores impeding heat transfer by conduction, convection, and radiation [3]. As a key heat transfer parameter, effective thermal conductivity can directly evaluate the thermal insulation performance of porous materials [4]. Furthermore, discerning the relationship between the internal structure and the effective thermal conductivity can provide valuable insights for the structural design and optimization of thermal insulators. Consequently, the prediction of the effective thermal conductivity of realistic porous materials offers a substantial theoretical foundation for the advancement of thermal insulation materials.

Traditional methods, based on theoretical models and numerical simulation, are usually employed to obtain effective thermal conductivity of porous media. The Maxwell-Garnett (M-G) model [5], a classic

effective medium theory model, is primarily utilized for predicting the effective thermal conductivity of composite materials containing particulate phase materials. The model assumes that the continuous phase is homogeneous, isotropic, and linear, and the discrete phase is also homogeneous and isotropic, dispersed in the continuous phase in a spherical form [6,7]. By establishing a heat conduction differential equation and incorporating corresponding boundary conditions, the effective thermal conductivity of the composite material can be derived. The M-G model, being mathematically simple, facilitates quick and convenient prediction of the effective thermal conductivity of composite materials, providing theoretical guidance for material design and circumventing extensive experimental work. However, due to certain simplified assumptions such as the idealization of particle shape and dispersion state, there may be some deviation between the predicted value and the experimental measurement value. To address this issue, Bruggeman et al. proposed a novel model, known as the Bruggeman model [8]. The distinctive feature of this model is that it does not explicitly distinguish between the continuous phase and the discrete phase, making it more adaptable to many practical composite materials where both phases are continuous. The fundamental concept of the Bruggeman model is to consider the composite material as a symmetric

* Corresponding authors.

E-mail addresses: longdh@mail.ecust.edu.cn (D. Long), yy.zhang@ecust.edu.cn (Y. Zhang).

mixture of two media, i.e., after the two phases are mixed, the effective thermal conductivity of the new material should ensure the continuity of the heat flow between the phases. Based on this concept, we can establish a thermal equilibrium equation and derive the formula for the effective thermal conductivity. However, it should be noted that this model is based on certain simplifying assumptions, and therefore, it does not take into account the effects of interface effects, shape, and dispersion on the effective thermal conductivity [9]. The Lattice Boltzmann Method (LBM) offers an efficient approach to account for microscopic factors such as shape dispersion effects [10]. This method starts directly from the microscopic structure, eliminating the need for simplifying assumptions, and provides a more comprehensive consideration of interface effects, shape effects, and aggregation dispersion effects. The LBM establishes a discrete lattice model and defines the Boltzmann distribution function at each node. It constructs a Boltzmann equation to describe the evolution of the distribution function and defines the correspondence between macroscopic thermal parameters and microscopic distribution. The effective thermal conductivity is obtained through simulation calculations. However, the method involves large computational loads and demands on the convergence, stability, and computational error of the algorithm itself, making implementation complex. Additionally, the coupled description of fluid dynamics and thermodynamics is also complex, increasing the difficulty of model establishment [10,11].

In recent years, the rapid development of computational capabilities and machine learning has propelled thermal conductivity studies of composite materials. These studies leverage technologies such as neural networks and support vector machines to establish relationships between material microstructure characteristics and effective thermal conductivity. Machine learning can handle more complex and implicit patterns without the need for explicit understanding of physical mechanisms, thereby avoiding the simplification of structures and parameters in traditional computational methods. Bao et al. compared different machine learning methods such as support vector machines, Gaussian regression models, to predict thermal conductivity [12], and found that machine learning methods can acquire porous materials thermal conductivity more rapidly and effectively compared to traditional approaches. However, prediction accuracy of machine learning is constrained by the dataset limitations, thus impeding high precision predictions. Later, the same group characterized the pore characteristics and shapes inside the structure by defining descriptors with physical meaning and then used traditional machine learning techniques to establish a model between structure and thermal conductivity performance [13]. To better describe structural shapes, Fei et al. [14] viewed granular materials as a network, where nodes in the network represent grains and edges represent contacts between particles. Based on complex network theory, they quantified key microstructural parameters of the granular structure, then used a neural network (NN) model trained to accurately predict the effective thermal conductivity. This study demonstrated that incorporating multiscale microscale parameters can enhance the precision of heat conduction predictions. However, the research was confined to dry granular materials, indicating that further investigation is required to determine its applicability to wet sands. Nevertheless, traditional machine learning approaches like Gaussian regression and support vector machines demand defining physical descriptors of material structural characteristics to correlate with thermal conductivity, which demands extensive tedious work and still fails to fully characterize all the intricate details inside the structure. Deep learning methods employ convolutional kernels that can operate directly on images or three-dimensional structures of materials [15,16], automatically learning latent features in the data without the need for manual crafting of feature descriptors. This overcomes the data pre-processing bottleneck faced by traditional machine learning approaches and reduces the complexity of steps involved in developing predictive models [17]. Du et al. established an accurate relationship model between the microstructure and effective thermal conductivity of sintered

silver through two-dimensional Scanning Electron Microscope (SEM) microstructure images and deep learning methods. It demonstrated that deep learning methods have higher precision in predicting effective thermal conductivity compared to traditional machine learning approaches [18]. Deep learning methods also have a defect in that they are essentially black box models and cannot explicitly express the specific form of the prediction model, lacking interpretability for the result prediction process [19].

To this end, we propose a novel deep learning approach that achieves this by correcting the material structure. We establish the structure-activity relationship between three-dimensional structures and thermal conductivity using a three-dimensional convolutional neural network (3D-CNN). To address the opacity issue of the prediction model, we employ Class Activation Mapping (CAM) [20], an interpretable machine learning technique, to gain a deeper understanding of the influence of the internal structure of porous materials on effective thermal conductivity. The heat and mass transfer processes in porous materials are regulated by a series of complex mechanisms, the extent of which largely depends on the complexity of the material's microstructure [21–24]. The intricate geometry of the pores makes the analysis of these transport phenomena extremely challenging, especially when multiple mechanisms are at play simultaneously [24]. The accuracy of the actual structure reconstruction of materials is crucial for predicting effective thermal conductivity [25–27]. Notably, previous methods presuppose that the material's structure is reasonable, or that the defined structural parameters can comprehensively describe its characteristics. The final effective thermal conductivity is obtained through the improvement of algorithms and the error and performance of the model itself, and these methods cannot identify, and correct errors related to the unreasonableness of the material structure. This study proposes a new process and method for the effective thermal conductivity of composite materials with a feedback mechanism. It provides intuitive visual effects, demonstrating how the complex internal pore structure affects the prediction of effective thermal conductivity. Then, through interpretable heat maps, a refined 3D structure and improved prediction of effective thermal conductivity are obtained. Feedback enables the simultaneous optimization of data and models. This interpretability provides guidance for future structural optimization and physical model development.

2. Methods

The overall workflow of the present study, as depicted in Fig. 1, encompasses three parts:

- (1) Dataset Construction: The primary objective of this segment is to construct a large-scale dataset to cater to the training needs of deep learning methodologies. As illustrated in Fig. 1(a), slices with porosity ranging from 10 % to 90 % are selected to reconstruct the detailed and accurate pore structure at the microscopic level for different porosities, utilizing the generator of a Generative Adversarial Network (GAN). Subsequently, the effective thermal conductivity corresponding to each porous material is obtained through the Porous Microstructure Analysis (PuMA) method. This approach facilitates the construction of a dataset for training the three-dimensional convolution model.
- (2) Deep Learning Model Training: In this segment, a three-dimensional convolutional neural network is designed without the addition of pooling layers, and a global average pooling layer is employed, followed by hyperparameter tuning. Through learning and training on the dataset, a high-precision model for effective thermal conductivity is achieved.
- (3) Interpretable Framework with Feedback Mechanism: The Class Activation Mapping (CAM) is employed to generate a heatmap that reflects the contribution to the final thermal conductivity by taking the weighted sum of the last convolutional layer. This

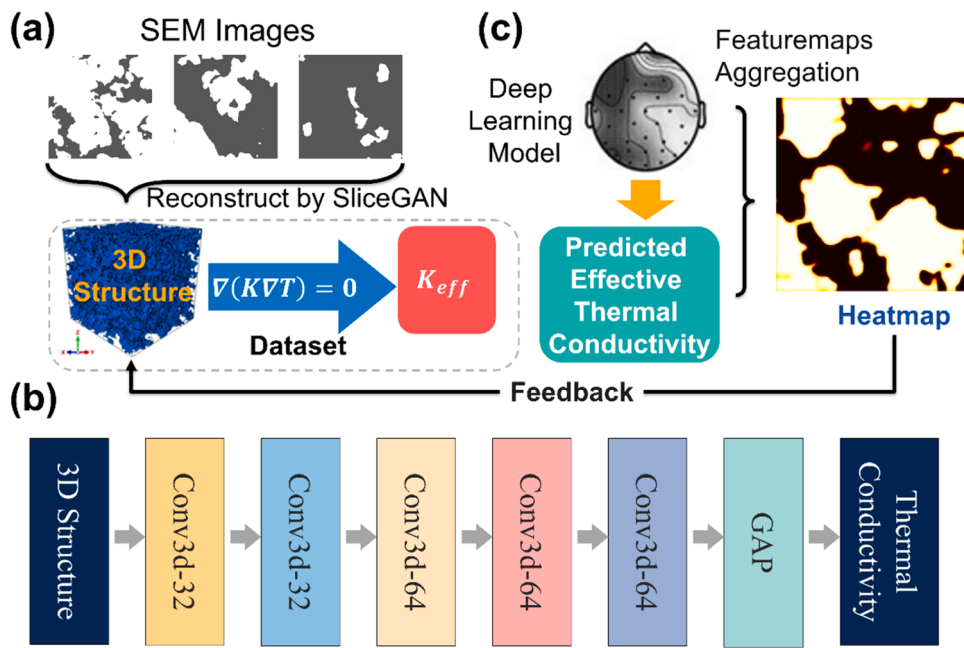


Fig. 1. The overall workflow of explainable machine learning for predicting effective thermal conductivity (a) Construction of dataset through 2D SEM images and solution of heat transfer equation (b) Training of fully convolutional neural network (c) Model prediction of effective thermal conductivity and generation of thermal maps.

heatmap provides an intuitive understanding of the relationship between structure and thermal conductivity. Furthermore, it is observed that the errors existing in the original three-dimensional structure are fed back to the dataset to enhance the rationality of the model, ultimately yielding a more realistic thermal conductivity.

2.1. Generation of dataset

The input part of the deep learning dataset in this work uses the SliceGAN developed by Steve Kench and Samuel J. Cooper to generate three-dimensional structures of porous materials [28]. The algorithm achieved balanced 3D structural information density through specific generator architecture design of the GAN network. This enabled SliceGAN to generate high-quality internal images across the 3D structure, compared to other generative algorithms, synthesizing high-fidelity internal details of porous materials. This is crucial for an in-depth study of the relationship between internal material characteristics and effective thermal conductivity.

Based on our previous work [29], the microstructural characteristics of aerogels were meticulously analyzed using scanning electron microscopy. This analysis yielded two-dimensional binarized slice images of varying porosities, which were obtained through a sophisticated image pre-processing technique implemented with Python's OpenCV package. The GAN was trained on these images, optimizing the loss function via gradient descent and utilizing internal feature statistics. This process resulted in the generation of nine distinct weight files, each corresponding to porosities ranging from 10 % to 90 %. Utilizing these weight files, we were able to generate a substantial number of three-dimensional structures of porous materials, each exhibiting realistic internal details.

The output part of the deep learning dataset in this work uses the PuMA [30] software developed by the National Aeronautics and Space Administration (NASA) to calculate the effective thermal conductivity of porous materials. Heat conduction equation was solved using the finite element method. For all microstructures, a unit temperature difference (1 K) was applied on the relative surfaces along the simulated axial

direction, while periodic boundary conditions were imposed on the remaining surfaces. The thermal conductivities of the solid and pore phases were 0.2 and $0.023 \text{ W}\cdot\text{m}^{-1}\cdot\text{K}^{-1}$ respectively.

In calculating thermal conductivity, PuMA solves the steady-state heat diffusion equation based on harmonic averaging and explicitly introducing jump conditions across material interfaces. The material is defined as a discrete system in the following formula by the boundary position information and state of the material.

$$\begin{bmatrix} \frac{2}{h^2} & \frac{1}{h^2} & \frac{1}{h^2} & -\frac{1}{2h} & -\frac{1}{2h} \\ \frac{1}{h^2} & -\frac{2}{h^2} & \frac{1}{h^2} & 0 & -\frac{1}{2h} \\ \frac{1}{h^2} & \frac{1}{h^2} & -\frac{2}{h^2} & -\frac{1}{2h} & 0 \\ -2\frac{(\beta_1 - \beta_2)}{(\beta_1 + \beta_2)h} & 0 & 2\frac{(\beta_2 - \beta_1)}{(\beta_1 + \beta_2)h} & 1 & 0 \\ 2\frac{(\beta_2 - \beta_1)}{(\beta_1 + \beta_2)h} & -2\frac{(\beta_1 - \beta_2)}{(\beta_1 + \beta_2)h} & 0 & 0 & 1 \end{bmatrix} \bullet \begin{bmatrix} u_1 \\ u_2 \\ u_3 \\ J_1 \\ J_2 \end{bmatrix} = \begin{bmatrix} 0 \\ 0 \\ 0 \\ -2\frac{(\beta_1 - \beta_2)}{(\beta_1 + \beta_2)h} \\ 2\frac{(\beta_2 - \beta_1)}{(\beta_1 + \beta_2)h} \end{bmatrix} \quad (1)$$

Where h represents the boundary distance, β_1 and β_2 represent the intrinsic thermal conductivity of the solid and medium, respectively. u_1 , u_2 and u_3 are unknown values at 1/6, 3/6 and 5/6, respectively. J_1 and J_2 represent the derivatives from the two jumps u_1-u_2 and u_2-u_3 on the interface. By solving the matrix of the discrete system, the effective thermal conductivity β^* of the overall porous material is finally obtained, as shown in the following formula:

$$\beta^* = \sum_i^n \left(\frac{u_{i+1} - u_{i-1}}{h} - \frac{1}{2} [\partial_x u]_{i+\frac{1}{2}} + \frac{1}{2} [\partial_x u]_{i-\frac{1}{2}} + 1 \right) \beta_i h \quad (2)$$

2.2. Three-dimensional convolutional neural network

Three-dimensional Convolutional Neural Networks (3D CNNs) demonstrate significant advantages in predicting the thermal conductivity of porous materials, primarily by extracting features from three-dimensional structures. As the number of network layers increases, 3D CNNs are capable of capturing complex features that are more relevant to effective thermal conductivity. Notably, 3D CNNs directly process three-dimensional structures without the need to unfold them into two-dimensional slices, greatly reducing the workload of image pre-processing. In addition, three-dimensional convolution can extract three-dimensional spatial features and hierarchical information. Compared to a single two-dimensional slice, it can capture a richer overall structural representation. This characteristic makes it possible to model the structure-thermal conductivity relationship more accurately. On the other hand, the number of parameters in 3D CNNs is relatively small, which reduces the risk of overfitting, especially on small datasets. In summary, 3D CNNs, by learning directly from three-dimensional structures, predict thermal conductivity in an efficient and scalable manner, demonstrating significant advantages. However, there are still some details that need further discussion:

Fully convolutional neural network architecture. The primary objective of the pooling layer is to reduce the dimensionality of features, thereby decreasing computational complexity and preventing overfitting in neural networks [20]. However, the pooling layer aggregates pixels or features to achieve this reduction in feature dimensionality, inevitably leading to some loss of spatial information. As illustrated in Supplementary Fig. S1, applying a $2 \times 2 \times 2$ pooling operation with a stride of 1 to a $320 \times 320 \times 320$ three-dimensional structure results in a halving of its dimensions. More importantly, internal features are gradually lost through successive pooling operations. From the perspective of predicting the effective thermal conductivity of materials, these details present in the spatial domain will influence the final thermal conductivity results. Furthermore, spatial location information is required when generating heat maps. Therefore, in the design of convolutional neural networks for high-precision prediction of thermal conductivity, the use of pooling layers is not advisable.

Global average pooling (GAP) layer replaced the fully connected layer. Compared to fully connected layers, Global Average Pooling (GAP) layers demonstrate superior adaptability in mapping high-dimensional features to effective thermal conductivity [31], primarily based on the following two key factors: Firstly, fully connected layers introduce a large number of parameters, which may lead to model overfitting, especially in cases of small sample sizes. In contrast, GAP layers do not have trainable parameters, which helps mitigate the risk of overfitting and enhances the model's generalization capability. Secondly, GAP layers are capable of preserving spatial information within feature maps. This is crucial for predicting effective thermal conductivity, as the spatial distribution of the internal structure of materials can impact heat transfer performance. Fully connected layers, however, lose this spatial information during the mapping process. GAP layers reduce dimensionality by averaging feature maps, while simultaneously preserving all spatial information, which is essential for subsequent heat map generation. Essentially, the role of the GAP layer can be more accurately described as aggregating the complete spatial information of the feature map into a point. These points form a vector, establishing a mapping relationship between the feature map representation and the final output result. The weights of each point on the output result are obtained from the linear mapping from the GAP layer to the output. These weights indicate the degree of influence of the feature maps extracted from the final convolutional layer on the effective thermal

conductivity.

2.3. Generation of heatmaps

Heat maps significantly enhance the transparency and interpretability of convolutional neural networks. Through heat maps, we can intuitively observe the impact of the internal morphology of the three-dimensional structure of porous materials on the effective thermal conductivity results. As shown in Fig. 2, it is the basic process of generating heat maps. The main function of the convolution kernel is to extract the internal features of the three-dimensional structure that affect the effective thermal conductivity. As the number of convolution layers increases, the features extracted by the convolution layer become more and more prominent.

As shown in Fig. 2. The hook method in Pytorch is utilized to extract feature maps from the final convolutional layer. Subsequently, these feature maps undergo pooling through a GAP layer, where each node in the GAP layer represents a feature map. Therefore, by employing the net.parameters method in Pytorch, a Python library, parameters of the network's final layer can be retrieved, thereby determining the influence weights of each feature map on the effective thermal conductivity results. Finally, the weighted sum of each feature map and its corresponding weight is computed to obtain the final heat map.

3. Results and discussion

3.1. Building the dataset

GAN generators with various parameters were trained based on the two-dimensional slicing method from previous work [29]. These trained generators could produce nine 3D structures with porosities ranging from 10 % to 90 %, as depicted in Fig. 3.

The dimensionality of the noise vector plays a pivotal role in determining the size of the generated three-dimensional structure. A structure that is too small fails to capture sufficient internal structural details, while an overly large structure incurs significant computational costs and may lead to instability in the generated results. By statistically analysing the deviation between the three-dimensional structures generated by five different sizes of noise vectors and the actual SEM slice images (as shown in Fig. 4(b)), we found that the structure of size 192 exhibited the smallest error, thus being selected as the optimal size. Although the structure of size 288 showed a slightly lower median error, size 192 is considered to be the optimal dataset size due to its higher computational efficiency. In essence, a dataset size of 192 allows for the construction of high-quality, low-error three-dimensional porous structures while maintaining reasonable computational overhead. This contributes to the establishment of a more accurate structure-performance relationship model.

Finally, utilizing the SliceGAN and PuMA techniques, we have successfully constructed a dataset encompassing 16,690 three-dimensional structures of porous materials along with their corresponding effective thermal conductivities. To evaluate the ultimate performance of the deep learning model, we have additionally generated a test dataset comprising 1000 samples. These achievements not only enrich the structural database of porous materials but also provide crucial experimental data for the prediction of thermal conductivity.

3.2. Obtaining high-precision predictive model

In order to achieve a model with robust generalization and predictive capabilities, we adjusted the number of convolutional layers in the fully convolutional neural network. Initially, we investigated the impact of dataset size on network performance. The dimensions of the convolutional filters were first specified as $3 \times 3 \times 3$. A stride of 1 and padding of 1 were determined to ensure consistency in image dimensions post-convolution. Subsequently, we explored the performance of models

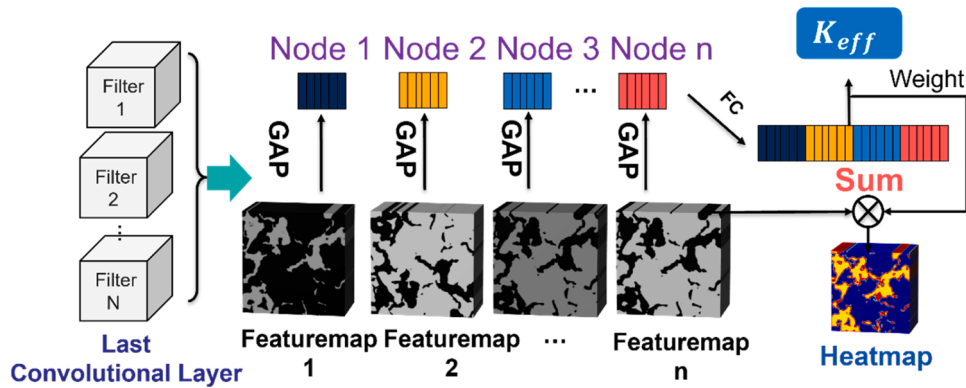


Fig. 2. The methodology of heatmap visualization.

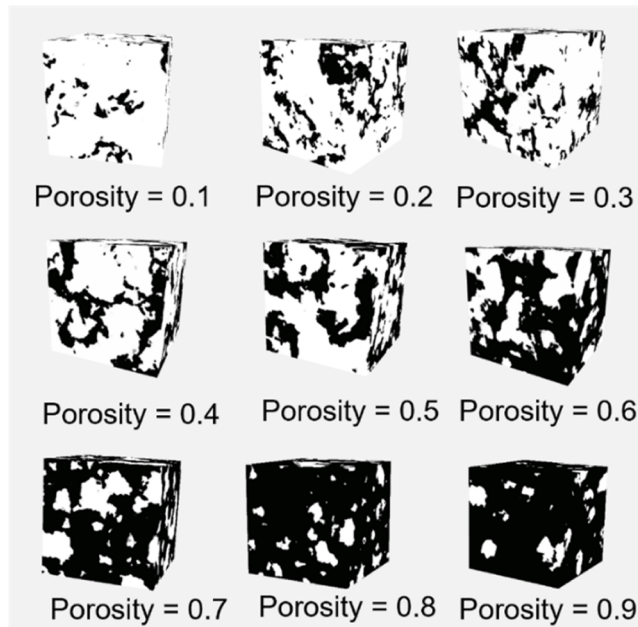


Fig. 3. Three-dimensional structures of porous materials with nine distinct porosity parameters.

with varying numbers of convolutional layers and different numbers of kernels per layer. As shown in Fig. 5(a), as the model complexity increases, the training error of the model gradually decreases. However, the validation error representing the generalization ability shows a slightly upward trend. This is because an overly complex model can lead to overfitting on the training set and performance degradation on the validation set. Therefore, to achieve a model with robust generalization capabilities, both training and validation errors were taken into account when selecting model parameters. After comprehensive consideration, five convolutional layers and an appropriate number of convolutional filters were selected. The final architecture of the 3D convolutional neural network consisted of 32, 32, 64, 64, and 64 convolutional kernels in each layer, respectively, to strike a balance between model complexity and generalization capability.

In addition, the effect of dataset size on model performance was also evaluated to determine the influence of data size on model performance. As shown in Fig. 5(b), as the size of the dataset increases, both the training and validation errors of the model decrease rapidly, eventually stabilizing around a dataset size of 12,000. This trend suggests that fully convolutional neural networks are capable of learning from the dataset with minimal noise interference. Furthermore, taking into account computational resources and the model's fitting capability, an optimal dataset size is determined to be approximately 12,000. Smooth L1 Loss function as shown in the following formula was selected.

$$\text{SmoothLoss} = \begin{cases} -0.5(\hat{y} - y)^2, & |\hat{y} - y| < 1 \\ |\hat{y} - y| - 0.5, & |\hat{y} - y| \geq 1 \end{cases} \quad (3)$$

Where \hat{y} represents the estimated value of the model, and y is the actual value. The benefit of choosing the SmoothL1 function is that it can

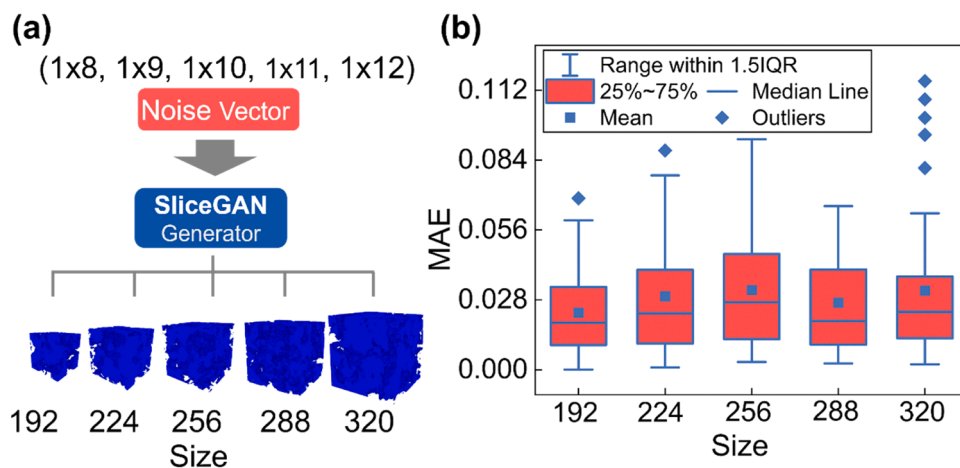


Fig. 4. (a) Generating variably sized structures by tuning the noise vector (b) Box plot of errors in generated three-dimensional structures of varying sizes.

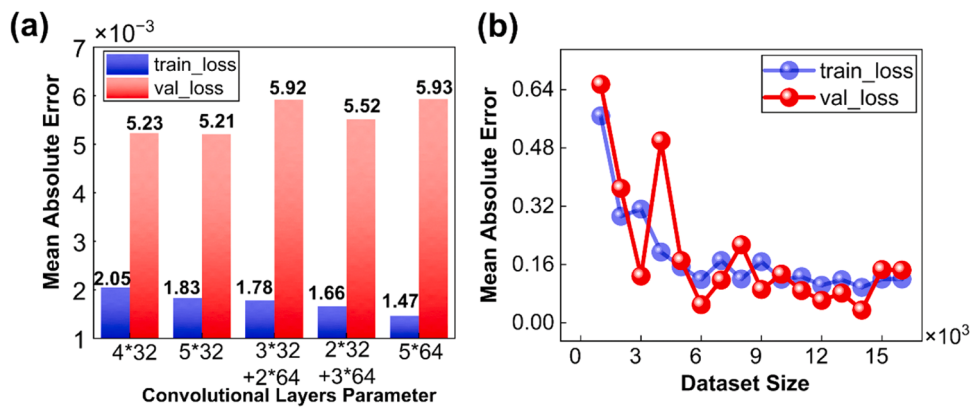


Fig. 5. (a) Training and validation error of model with different convolution layer parameters. (b) The impact of dataset size on model performance.

reduce excessive punishment for small errors, avoid gradient disappearance, and provide a smoother loss landscape. This helps the stable training and convergence of the model. Stochastic Gradient Descent (SGD) was chosen as the optimization method, incorporating an L2 regularization term of 10^{-5} and a momentum of 0.9. The initial learning rate was set to 10^{-4} , and an exponential decay learning rate update strategy was chosen. The advantage of this method is that the larger initial learning rate can quickly exceed saddle points and local optima to find better solutions. The subsequent learning rate decay causes the model to oscillate around better solutions and gradually stabilize, thereby helping to jump out of saddle points and local optima to find globally optimal parameters. First, the larger initial learning rate can accelerate the convergence of early training, and the subsequent gradual decay can reduce the risk of overfitting during training. The selected momentum can further accelerate training by incorporating information

from the forward gradient into the current update step. Through rapid initial progress and limited local fine-tuning, global optimal solutions are more easily identified. In summary, the specified algorithm and parameters meet the goals of promoting model optimization and improving generalization.

3.3. Prediction effective thermal conductivity

As shown in Fig. 6(a), the training error of the 3D CNNs steadily decreases during the iterative training process. Despite initial fluctuations in the validation error, it converges with the training error after the 40th iteration, indicating that the model has achieved a relatively high level of accuracy in predicting both the training set and unseen data. In addition, we used an additional 1000 test datasets to evaluate the predictive capabilities of the Maxwell, Bruggeman, and 3D CNN models.

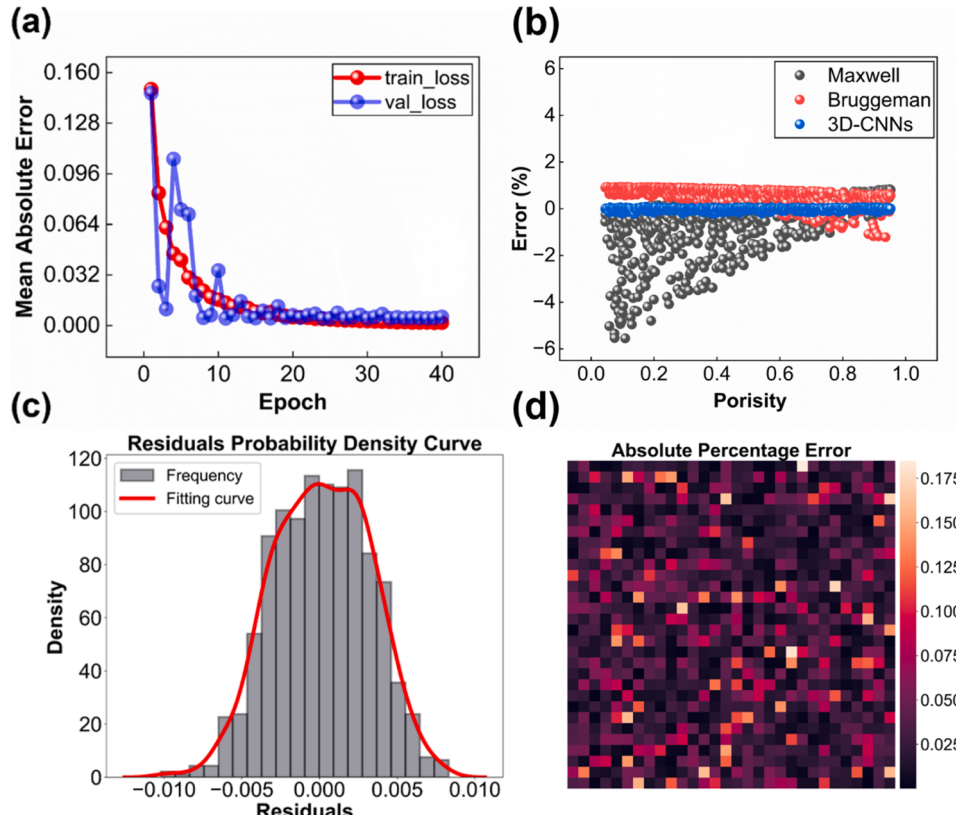


Fig. 6. (a) The training process of the 3D convolutional neural network (b) Performance of different models in predicting the effective thermal conductivity error (c) Probability density distribution of model prediction residuals (d) Distribution of median absolute percentage error of model prediction.

Fig. 6(b) shows the error between the predicted and actual values of these three models. From the figure, it can be seen that the performance of the Maxwell model is not as good as the other two models, especially at high porosity, where the Bruggeman model produces a larger error. Overall, the predictive performance of the 3D convolutional neural network model far exceeds that of traditional numerical models, with a prediction accuracy of 96.47 % on the test set and a variance of 10^{-5} (see Supplementary Material Fig. s3). **Table 1** provides a detailed comparison of the predicted and actual values for six different pore structures. Through in-depth analysis of the numerical data, we found that the difference between the predicted and actual values is negligible, indicating minimal bias. This result strongly suggests that our deep learning model exhibits very high accuracy and reliability in predicting the effective thermal conductivity of materials.

To evaluate the reliability of the model, we conducted an uncertainty analysis and calculated the variance and median absolute percentage error (APE) of the predicted and actual values for all test set data (**Eq. (4)**). APE by calculating the absolute value to avoid the cancellation of positive and negative errors, better reflects the stability of overall prediction accuracy. **Fig. 6(c)** shows the probability density curve of residuals, which provides insight into the characteristics of prediction errors and model bias. The shape of the fitted curve is very similar to a normal distribution, indicating that most prediction errors are small and only a few show larger errors. This bell-shaped curve indicates that positive and negative prediction errors are relatively balanced, with no obvious systematic bias. The closeness to a normal distribution also indicates that the prediction model has good generalization performance and can capture potential patterns well. **Fig. 6(d)** shows that the median error of the predicted effective thermal conductivity remains at a low level, with an average of about 0.025 for different test sets, indicating that the model's prediction results have small and evenly distributed errors, and the prediction accuracy of effective thermal conductivity is stable.

$$APE = \frac{|\hat{y} - y|}{\max(\epsilon, y)} \quad (4)$$

3.4. Analysis of the importance of internal material characteristics

To evaluate whether the deep learning model can effectively learn the relationship between the three-dimensional structure and the effective thermal conductivity, we performed a voxel value distribution analysis of the heat maps of the three-dimensional structures with porosity ranging from 10 % to 90 %. The voxel values reflect the degree of influence of each position in the three-dimensional structure space on the effective thermal conductivity, and the higher the voxel value, the greater the influence. As shown in **Fig. 7**, the distribution of the heat maps exhibits a distinct bimodal feature, indicating that the model can accurately identify the three-dimensional structure regions that affect the effective thermal conductivity. The bimodal distribution suggests that the model considers that there are two regions in the three-dimensional structure space that have a significant impact on the effective thermal conductivity. This demonstrates the rationality of the data and training process used by the model, as well as the model's learning ability of the relationship between structure and performance.

Subsequently, the factors influencing the effective thermal conductivity within the material were intuitively revealed through heat maps. As shown in **Fig. 8(a)**, a series of heat maps corresponding to continuous slices of the three-dimensional structure are presented. These heat maps provide an intuitive visual tool that clearly shows the degree of influence at each location on different cross-sections. In the heat map, the voxel value at each location represents the degree of influence of that location on the effective thermal conductivity. Voxel value at each position in the heatmaps denotes the magnitude of its effect on the effective thermal conductivity. Larger voxel values (brighter colors in that region) correspond to greater influence, while smaller voxel values (darker colors) indicate less influence. And **Fig. 8(b)** presents a magnified heatmap, facilitating further discussion on the results of the heatmap.

Table 1
Comparison of predicted values and ground truth values.

3D Structure			
Ground Truth	0.00950	0.07659	0.12132
Prediction	0.00929	0.07809	0.12351
3D Structure			
Ground Truth	0.10246	0.14767	0.085340
Prediction	0.10636	0.15339	0.085724

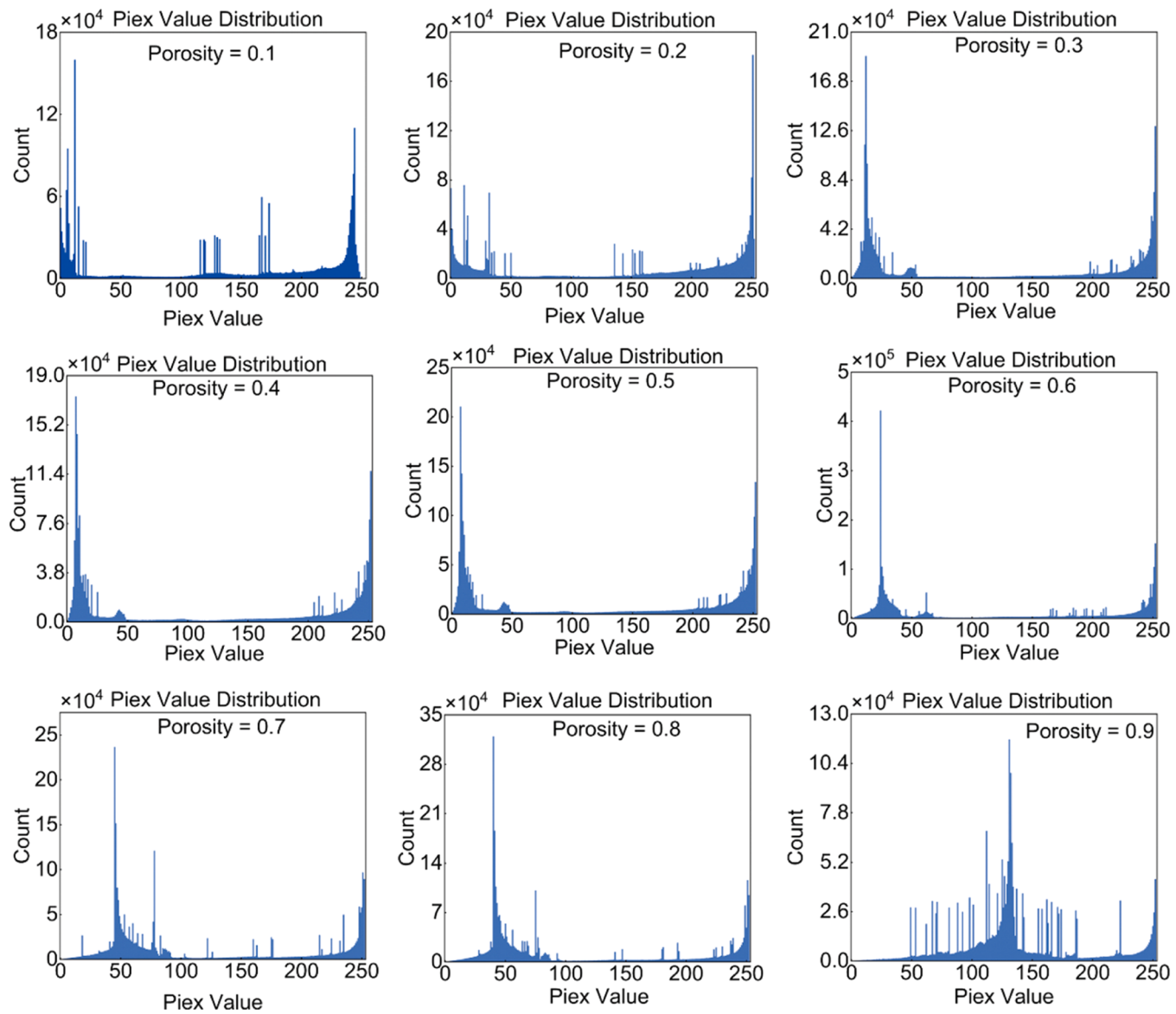


Fig. 7. Voxel distribution in heatmaps at different porosities.

According to the heatmaps, the following conclusions were reached: The measured effective thermal conductivity indicates that the microscopic structure and related heat transfer mechanisms of porous materials have a significant effect on their effective thermal conductivity. Particularly, as shown in Fig. 8(b), the irregular interface between the solid and the surrounding medium, marked by the green circle, has the most significant impact on the effective thermal conductivity. This effect is especially prominent in areas where the solid matrix and the medium contact in complex ways. This result is consistent with our understanding of the physical mechanism of heat transfer, that is, the main heat transfer occurs in more complex pore areas. In high porosity areas, turbulent heat transfer and radiative heat transfer mechanisms are more pronounced, thus having a greater impact on effective thermal conductivity. In addition, as shown in the white box area, independent small solid particles also have a significant impact on thermal conductivity. Overall, the thermodynamic analysis well explains the influence mechanism of the internal microstructure of the material on the effective thermal conductivity from the perspective of heat transfer mechanism.

The calculation results of the heatmap provide a theoretical basis for the design and prediction of high-performance porous materials. Firstly, from a microscopic perspective, the irregular contact of the solid

interface with the surrounding medium and the small solid particles enhance heat diffusion and turbulence, suppressing the orderly heat flow, thereby reducing the overall thermal conductivity of the material. This result validates the design concept of functionally graded porous materials, that is, by finely controlling the morphology and distribution of interfaces and pores, thermal transmission performance can be optimized. Secondly, from the perspective of 3D reconstruction and deep learning, the original 3D image contains only two voxel values (solid phase and medium), but actually contains some non-physical areas, such as the discrete fine particles in the medium space shown in the white box of Fig. 8(b), which is unreasonable for the actual porous materials and will produce minor errors. In the original image, it is difficult to identify and remove fine particles due to the discontinuous voxel values between fine particles, solids and matrix. In contrast, the generated thermal conductivity mapping considers the different effects of fine particles and solid matrix on effective thermal conductivity. Simple image threshold segmentation can easily identify and remove non-physical areas such as fine particles, thereby obtaining a more accurate three-dimensional structure.

Furthermore, through the feedback of such effective thermal conductivity results, the dataset itself can be corrected to obtain the true

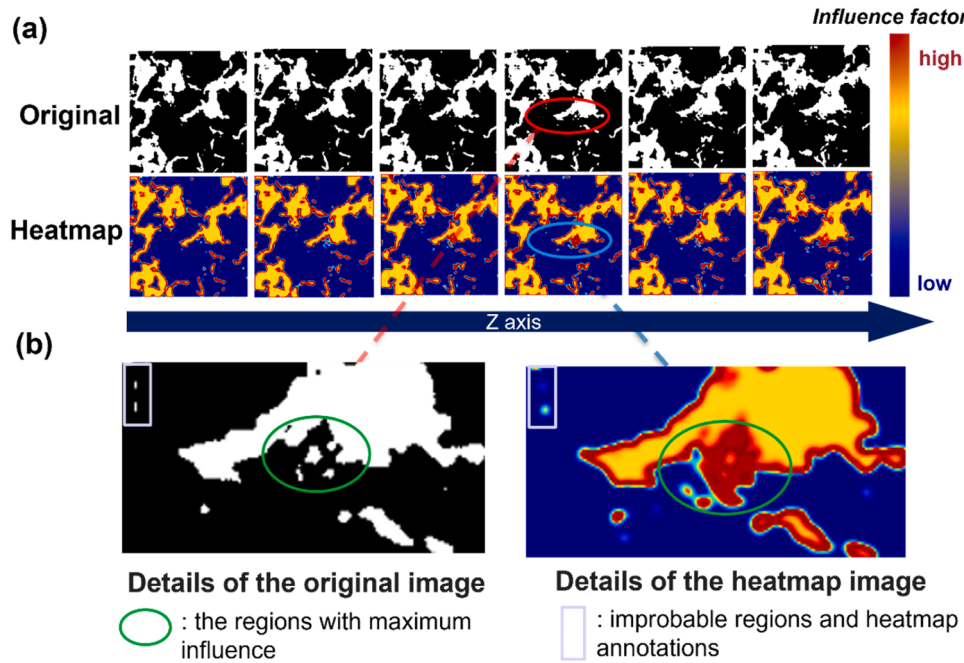


Fig. 8. (a) Serial slices of 3D structure and heatmaps. (b) Details of heat maps upon magnification.

three-dimensional structure and effective thermal conductivity of porous materials. Through iterative feedback of results and correction of datasets, the prediction accuracy can be continuously improved.

To this end, by simple threshold segmentation method (threshold of 125 in this work) to process the thermal map and identify and eliminate unreasonable areas and parts in the original 3D structure. As depicted in Fig. 9(b) and (c), the thermal map allowed visual observation of the tiny and suspended particles captured within the 3D structure, which were subsequently eliminated via threshold segmentation. In addition, the two-point correlation function of the 3D structure was calculated before and after the correction. The two-point correlation is a statistical measure used to evaluate the probability of two points appearing in the same phase in a medium, which can well reflect characteristics of the 3D

structure such as connectivity, uniformity, dependence, and complexity [32]. As shown in Fig. 9(a), the corrected structure showed more stable and realistic two-point correlation performance, which is closer to that of real porous materials. Therefore, the feedback from the thermal map can effectively reduce the error of the dataset itself, resulting in a more accurate thermal conductivity of porous materials. The thermal map allowed us to identify and correct unreasonable areas in the original 3D structure, improve the two-point correlation performance, which provided a simple and effective means to improve the accuracy of thermal conductivity prediction. The changes in porosity and thermal conductivity of the porous material structure before and after correction are shown in Table 2.

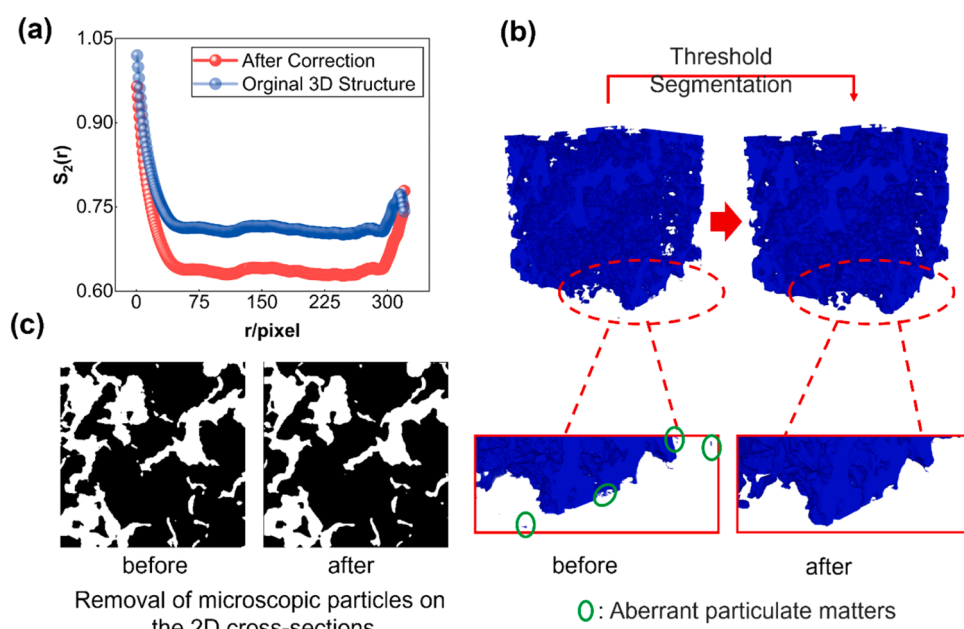


Fig. 9. (a) Expression of the correlation between two points before and after correction (b) Visual correction of the 3D structure (c) Correction on the cross-sectional slices of the 3D structure.

Table 2

Porosity and effective thermal conductivity of porous materials before and after correction.

Porous materials	Porosity (%)		Effective thermal conductivity (W/m·K)	
	before	after	before	after
Sample 1	65.580	69.348	0.06850	0.06485
Sample 2	76.162	79.990	0.05615	0.05394
Sample 3	59.390	60.113	0.05656	0.05431
Sample 4	54.790	59.574	0.05577	0.05333
Sample 5	46.134	40.734	0.05545	0.05486

4. Conclusion

This study introduces a novel workflow that combines interpretable deep learning with feedback from prediction results for the prediction of effective thermal conductivity of porous materials. Our 3D convolutional neural network demonstrates exceptional accuracy in predicting effective thermal conductivity, with error distributions following a normal distribution, indicating high model stability. Furthermore, heat maps generated by our class activation mapping explainable method intuitively reveal the impact of internal pore structure characteristics on effective thermal conductivity, consistent with the physical mechanism of heat conduction. Through these heat maps, we identify and eliminate unreasonable suspended particles in the 3D structure, thereby obtaining a more refined material reconstruction model and further enhancing the accuracy and reliability of our predictions. In summary, this work provides intuitive visual effects, demonstrating how complex internal pore structures influence the prediction of effective thermal conductivity, thereby improving the precision of model reconstruction and prediction. Although our method is currently only used for predicting effective thermal conductivity, this workflow that combines interpretable learning and feedback has tremendous potential in the modeling of structure-property relationships in the field of materials science. Future work can study key parameters such as solid-phase thermal conductivity, porosity, pore size distribution, and anisotropy, and apply the interpretable deep learning method to fully understand the structure-property relationship of porous materials, thereby guiding the design of thermal insulation materials.

Statement

In the research work, no AI tools were used to generate data and experimental results, and it was ensured that the authenticity of data results would not be affected in the process of generating text. The author is responsible for the authenticity of the results of the article.

Additional information

See the supplementary materials for the additional charts and program codes used in this article.

CRediT authorship contribution statement

Qingfu Huang: Conceptualization, Methodology, Software, Writing – original draft, Writing – review & editing. **Donghui Hong:** Data curation. **Bo Niu:** Software. **Donghui Long:** Conceptualization, Methodology, Funding acquisition. **Yayun Zhang:** Conceptualization, Methodology, Writing – review & editing, Funding acquisition.

Declaration of Competing Interest

The authors declare that they have no known competing financial interests or personal relationships that could have appeared to influence the work reported in this paper.

Data availability

Data will be made available on request.

Acknowledgements

This study was supported by the National Natural Science Foundation of China (nos. 22008073, 21878091, 22078100, and 52102098), Shanghai Sailing Program (no. 20YF1410600), Fundamental Research Funds for the Central Universities (JKD01221701), and Shanghai Talent Development Fund (2021026).

Supplementary materials

Supplementary material associated with this article can be found, in the online version, at [doi:10.1016/j.ijheatmasstransfer.2023.125064](https://doi.org/10.1016/j.ijheatmasstransfer.2023.125064).

References

- [1] R. Luque, A. Ahmad, S. Tariq, M. Mubashir, M. Sufyan Javed, S. Rajendran, R. S. Varma, A. Ali, C. Xia, Functionalized interconnected porous materials for heterogeneous catalysis, energy conversion and storage applications: recent advances and future perspectives, Mater. Today (2023), S1369702123001372, <https://doi.org/10.1016/j.mattod.2023.05.001>.
- [2] T.D. Bennett, F.X. Couder, S.L. James, A.I. Cooper, The changing state of porous materials, Nat. Mater. 20 (2021) 1179–1187, <https://doi.org/10.1038/s41563-021-00957-w>.
- [3] H.K.M. Al-Jothery, T.M.B. Albarody, P.S.M. Yusoff, M.A. Abdullah, A.R. Hussein, A review of ultra-high temperature materials for thermal protection system, IOP Conf. Ser. Mater. Sci. Eng. 863 (2020), 012003, <https://doi.org/10.1088/1757-899X/863/1/012003>.
- [4] S. Chongdar, S. Bhattacharjee, P. Bhanja, A. Bhaumik, Porous organic–inorganic hybrid materials for catalysis, energy and environmental applications, Chem. Commun. 58 (2022) 3429–3460, <https://doi.org/10.1039/D1CC06340E>.
- [5] I.A. Starkov, A.S. Starkov, Maxwell–Garnett model for thermoelectric materials, Int. J. Solids Struct. 202 (2020) 226–233, <https://doi.org/10.1016/j.ijсолistr.2020.06.023>.
- [6] R.H. Khiabani, Y. Joshi, C.K. Aidun, Thermal properties of particulate TIMs in squeeze flow, Int. J. Heat Mass Transf. 53 (2010) 4039–4046, <https://doi.org/10.1016/j.ijheatmasstransfer.2010.05.023>.
- [7] P.E. Okafor, G. Tang, Study of effective thermal conductivity of a novel SiO₂ aerogel composite for high-temperature thermal insulation, Int. J. Heat Mass Transf. 212 (2023), 124242, <https://doi.org/10.1016/j.ijheatmasstransfer.2023.124242>.
- [8] D.A.G. Bruggeman, Berechnung verschiedener physikalischer Konstanten von heterogenen Substanzen. I. Dielektrizitätskonstanten und Leitfähigkeiten der Mischkörper aus isotropen Substanzen, Ann. Phys. 416 (1935) 636–664, <https://doi.org/10.1002/andp.19354160705>.
- [9] D. Ding, Q. Zhang, G. Qin, Y. Chen, Offset supper-cell model of polymer composites with oriented anisotropic fillers for thermal conductivity prediction considering shape factor, Int. J. Heat Mass Transf. 214 (2023), 124373, <https://doi.org/10.1016/j.ijheatmasstransfer.2023.124373>.
- [10] Q. Shu, L. Pan, R. Kneer, M. Rietz, W. Rohlf, Effective thermal conductivity simulations of suspensions containing non-spherical particles in shear flow, Int. J. Heat Mass Transf. 204 (2023), 123808, <https://doi.org/10.1016/j.ijheatmasstransfer.2022.123808>.
- [11] R. Ruppin, Evaluation of extended Maxwell–Garnett theories, Opt. Commun. 182 (2000) 273–279, [https://doi.org/10.1016/S0030-4018\(00\)00825-7](https://doi.org/10.1016/S0030-4018(00)00825-7).
- [12] H. Wei, S. Zhao, Q. Rong, H. Bao, Predicting the effective thermal conductivities of composite materials and porous media by machine learning methods, Int. J. Heat Mass Transf. 127 (2018) 908–916, <https://doi.org/10.1016/j.ijheatmasstransfer.2018.08.082>.
- [13] H. Wei, H. Bao, X. Ruan, Machine learning prediction of thermal transport in porous media with physics-based descriptors, Int. J. Heat Mass Transf. 160 (2020), 120176, <https://doi.org/10.1016/j.ijheatmasstransfer.2020.120176>.
- [14] W. Fei, G.A. Narsilio, M.M. Disfani, Predicting effective thermal conductivity in sands using an artificial neural network with multiscale microstructural parameters, Int. J. Heat Mass Transf. 170 (2021), 120997, <https://doi.org/10.1016/j.ijheatmasstransfer.2021.120997>.
- [15] T. Cawte, A. Bazylak, A 3D convolutional neural network accurately predicts the permeability of gas diffusion layer materials directly from image data, Curr. Opin. Electrochem. 35 (2022), 101101, <https://doi.org/10.1016/j.colelec.2022.101101>.
- [16] A. Krizhevsky, I. Sutskever, G.E. Hinton, ImageNet classification with deep convolutional neural networks, Commun. ACM 60 (2017) 84–90, <https://doi.org/10.1145/3065386>.
- [17] V. Mallet, L. Checa Ruano, A. Moine Franel, M. Nilges, K. Druart, G. Bouvier, O. Sperandio, InDeep: 3D fully convolutional neural networks to assist *in silico* drug design on protein–protein interactions, Bioinformatics 38 (2022) 1261–1268, <https://doi.org/10.1093/bioinformatics/btab849>.

- [18] C. Du, G. Zou, Z. A. B. Lu, B. Feng, J. Huo, Y. Xiao, Y. Jiang, L. Liu, Highly accurate and efficient prediction of effective thermal conductivity of sintered silver based on deep learning method, *Int. J. Heat Mass Transf.* 201 (2023), 123654, <https://doi.org/10.1016/j.ijheatmasstransfer.2022.123654>.
- [19] P. Dutta, N.B. Muppalaneni, R. Patgiri, A survey on explainability: why should we believe the accuracy of a model? *Math. Comput. Sci.* (2020) <https://doi.org/10.20944/preprints202004.0456.v1>.
- [20] B. Zhou, A. Khosla, A. Lapedriza, A. Oliva, A. Torralba, Learning deep features for discriminative localization, (2015). <http://arxiv.org/abs/1512.04150> (accessed April 8, 2023).
- [21] B. Xiao, W. Wang, X. Zhang, G. Long, J. Fan, H. Chen, L. Deng, A novel fractal solution for permeability and Kozeny-Carman constant of fibrous porous media made up of solid particles and porous fibers, *Powder Technol.* 349 (2019) 92–98, <https://doi.org/10.1016/j.powtec.2019.03.028>.
- [22] B. Xiao, H. Zhu, F. Chen, G. Long, Y. Li, A fractal analytical model for Kozeny-Carman constant and permeability of roughened porous media composed of particles and converging-diverging capillaries, *Powder Technol.* 420 (2023), 118256, <https://doi.org/10.1016/j.powtec.2023.118256>.
- [23] M. Liang, C. Fu, B. Xiao, L. Luo, Z. Wang, A fractal study for the effective electrolyte diffusion through charged porous media, *Int. J. Heat Mass Transf.* 137 (2019) 365–371, <https://doi.org/10.1016/j.ijheatmasstransfer.2019.03.141>.
- [24] B. Xiao, Q. Huang, H. Chen, X. Chen, G. Long, A fractal model for capillary flow through a single tortuous capillary with roughened surfaces in fibrous porous media, *Fractals* 29 (2021), 2150017, <https://doi.org/10.1142/S0218348X21500171>.
- [25] K. Ogbuanu, R.V. Roy, Numerical computation of the effective thermal conductivity of two-phase composite materials by digital image analysis, *Int. J. Heat Mass Transf.* 197 (2022), 123377, <https://doi.org/10.1016/j.ijheatmasstransfer.2022.123377>.
- [26] A. Cecen, Material structure-property linkages using three-dimensional convolutional neural networks, *Acta Mater.* 146 (2018) 76–84.
- [27] X. Zhong, B. Gallagher, S. Liu, B. Kailkhura, A. Hiszpanski, T.Y.J. Han, Explainable machine learning in materials science, *npj Comput. Mater.* 8 (2022) 204, <https://doi.org/10.1038/s41524-022-00884-7>.
- [28] S. Kench, S.J. Cooper, Generating three-dimensional structures from a two-dimensional slice with generative adversarial network-based dimensionality expansion, *Nat. Mach. Intell.* 3 (2021) 299–305, <https://doi.org/10.1038/s42256-021-00322-1>.
- [29] D. Hong, Q. Huang, X. Xu, B. Chen, B. Niu, Y. Zhang, D. Long, Ascertaining uncertain nanopore boundaries in 2D images of porous materials for accurate 3D microstructural reconstruction and heat transfer performance prediction, *Ind. Eng. Chem. Res.* 62 (2023) 5358–5369, <https://doi.org/10.1021/acs.iecr.2c04602>.
- [30] J.C. Ferguson, F. Panerai, A. Borner, N.N. Mansour, PuMA: the porous microstructure analysis software, *SoftwareX* 7 (2018) 81–87, <https://doi.org/10.1016/j.softx.2018.03.001>.
- [31] M. Lin, Q. Chen, S. Yan, Network in network, (2014). <http://arxiv.org/abs/1312.4400> (accessed May 26, 2023).
- [32] K.Q. Li, Y. Liu, Z.Y. Yin, An improved 3D microstructure reconstruction approach for porous media, *Acta Mater.* 242 (2023), 118472, <https://doi.org/10.1016/j.actamat.2022.118472>.